Integration of disciplines in the structural analysis of historical constructions. The Monastery of San Jerónimo de Buenavista (Seville-Spain)

Margarita Cámara[a,*], Manuel Romero[a], Pablo Pachón[a], Víctor Compan[a], Paulo B. Lourenço[b]

[a] *Dept. of Continuum Mechanics, Universidad de Sevilla, Avenida Reina Mercedes, 41012 Sevilla, Spain*
[b] *Institute for Sustainability and Innovation in Structural Engineering, University of Minho, Guimaraes, Portugal*

Abstract

The assessment of the structural health of historical constructions is needed to carry out correct diagnoses and implement proper decision making strategies in the preservation built cultural heritage. In order to provide information about the state of different structural elements of the Monastery of San Jerónimo de Buenavista, in Seville (Spain), an extensive experimental campaign, mainly comprising non-destructive and in situ tests, was carried out. The present paper describes a structural analysis based on numerical models. The main goal of this research is to assess the improvement in the results of numerical model by integrating information from techniques which come from fields of knowledge that complement architecture and engineering, such as geophysics, archaeology or topography. A non-linear analysis under gravitational loads until reaching the ultimate load of the structure is developed. A model that is truer to the reality at a global level is obtained, highlighting significant improvements in the results at a local level.

Keywords:
multidisciplinary approach, historical constructions, experimental campaign, numerical model, non-linear analysis

1. Introduction

All built heritage recovery processes require the prior assessment of the structural state of such constructions. This assessment can be carried out by means of different techniques involving varying degrees of complexity, ranging from mere visual analyses to the extraction of material samples to be tested in laboratories.

Nowadays, the most valued techniques are those that are non-destructive or moderately destructive and respectful of this heritage, while also providing both reliable and valuable information regarding the structural behavior of a building. Likewise, the structural analysis of historical constructions using mathematical models has experimented significant advances over these past years [1]. These models can provide a large amount of information. However, it is difficult to develop them, given the high degree of uncertainty that exists regarding relevant factors in structural behavior [2]. Items such as the mechanical properties of constituting materials, which may

*Corresponding author.
Email address: mcamara@us.es (Margarita Cámara)

have deteriorated with the passing of time, the ground-to-structure relationship or the influence of the construction process undergone by a building, are for the most part unknown and should be incorporated into a structural model in order for it to accurately show the behavior of the actual structure.

The calibration of finite element models based on Ambient Vibration Testing (AVT) and Operational Modal Analysis (OMA) have gained a foothold over the past years as a method to achieve structural models that show a dynamic behavior matching that of the actual structure, which is obtained experimentally from the actual structure. The mechanical properties of materials are the parameters of the model that are generally updated using this technique. In this way, values based on experimental tests are obtained for parameters that are initially uncertain [3–6].

The dynamic identification of structures is a powerful tool which is able to provide reliable information regarding the behavior of the structure [7–9]. The main strengths of using techniques that apply this kind of information in the analysis of historical constructions reside in its non-destructive nature and in its capacity to also provide useful information to both determine and predict the damage state of the whole [6, 10].

However, the results obtained from the calibrated finite element models mentioned above may not correspond to the actual behavior of the structure at a local level [10], especially in historical buildings which, over time, have been subjected to varying events, uses, extensions, demolitions, etc., that have affected their structure.

In this sense, other non-destructive tests (NDT) or moderately destructive tests (MDT) are capable of providing information regarding the different structural elements that constitute a building complex. These techniques allow to identify aspects such as the internal composition of elements or the deterioration of materials and they sometimes come from other disciplines beyond architecture and civil engineering. Thus, non-destructive techniques such as those based on waves propagation (seismic tomography, georadar,...) are able to provide information about the internal composition of different elements or the level of degradation of their constituting materials. Other techniques, such as photogrammetry, that also has a non-destructive character, is able to show the strain state of the building. On the other hand, other types of techniques entail a more aggressive approach to the monument in order to provide useful information, as they usually require partially breaking or removing material. For example, inspection openings allow both to observe construction elements and to analyze them if samples from them are also extracted, the extraction of samples allows to perform lab tests that are able to determine parameters such as compressive strength and Young and Poisson moduli, and continuous samplings of foundations and soil provides information about both foundation materials and soil layers on which the foundations rest.

When the structural analysis process is based mainly on mathematical models, the results obtained from these tests are normally used as complementary information, that is, to validate or qualify those provided by the model itself. However, the information obtained can also be incorporated into the mathematical model in order for it to present results that are more in accordance with the actual behavior of the structure, not only at a global level, but also at a local level [11, 12]. During a structural analysis process, this would mean integrating other disciplines into the study, in addition to architecture and structural engineering.

In this paper, the structural analysis of the Monastery of San Jerónimo de Buenavista, in Seville, is presented. This analysis has been carried out based on a finite element model that was not only calibrated by using AVT and OMA, but also included information obtained from NDTs or MDTs performed by other fields of knowledge as a method to obtain a higher fidelity structural model of the building.

The construction of the Monastery of San Jerónimo began at the beginning of the fifteenth century. Nowadays, mainly the galleries of the main cloister and some parts of the church, like the tower, remain standing (Fig.1).

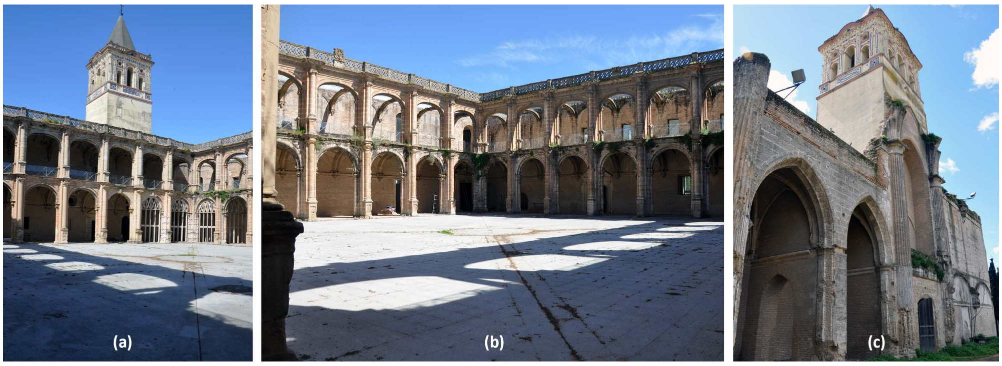

Figure 1: Views of the current state of the Monastery of San Jerónimo de Buenavista, Seville, Spain: (a) North and East wings and tower; (b) South and East wings; and (c) remains of the cloister church and the tower.

As for the Monastery's most recent history, it is important to emphasize two milestones. On one hand, the collapse of one of the columns of the northern wing of the cloister (rebuilt in 1973) as a result from the Portuguese earthquake of 1969 in the Gorringe bank between the Eurasian and African plates. On the other hand, the construction of a building attached to the remains of the southern and eastern wings of the cloister(2013) which currently houses a civic center (Fig.2).

Figure 2: Views of the civic center (a) under construction (2012) and (b) in service (2013).

After the construction of the new building, the existing damage in the cloister increased and it became urgent to assess the state of the entire complex. The Monastery is a building of significant size and it has a complex nature due to the numerous alterations it has suffered over the course of history, all of which have visibly affected its structure. However, this also enables the possibility of detecting localized deficiencies, making the Monastery a relevant case study to apply and validate the new approach of increasing the accuracy of a structural model by integrating information obtained from NDTs and MDTs.

The aim of the analysis presented in this paper is twofold: (i) to assess the improvement that a structural model of a historical construction can attain by means of the incorporation of information obtained from techniques with a non-destructive or a moderately destructive character, and (ii) to analyze the structural capabilities of the whole through a non-linear analysis, in order to both understand the behavior of the structure and establish a framework for future remedial interventions on the monument.

This paper is structured as follows. Section 2 contains a historical overview of the Monastery of San Jerónimo and a description of its current architectural configuration. Section 3 describes a set of inspection techniques carried out in the Monastery. Section 4 includes the development of the structural analysis model, which incorporates the results obtained applying the techniques identified in Section 3. Section 5 discusses the results obtained after the structural analysis based on the mentioned model. Finally, the main conclusions of this research are presented.

2. The Monastery of San Jerónimo de Buenavista

2.1. Historical aspects

Construction on the Monastery of San Jerónimo began in 1414 with the church. It was a gothic building with a main 45-meter-long nave, flanked by two wings with small chapels, an apse and a sacristy. During the first third of the sixteenth century, work on the church and the eastern cloister had finished, and the construction of the main cloister began, to the west, attached to the east cloister, over an ancient gothic cloister. This construction, built in renaissance style, was raised using calcarenite stone and was finished towards the end of that same century. The complex was completed by the middle of the seventeenth century, with the upper part of the tower and the printing house as the last additions [13] (Fig. 3.a).

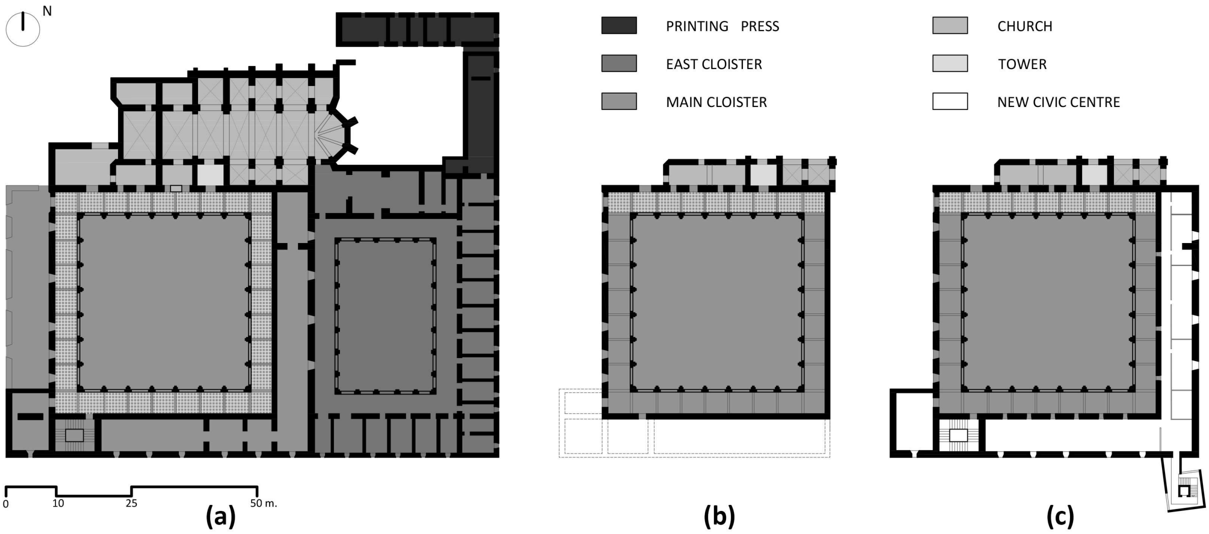

Figure 3: Historical evolution of the Monastery of San Jerónimo: (a) Original configuration, 1650; (b) historical remains, 2000; and (c) current architectural configuration of the complex, 2019.

The building was used as a monastery until the beginning of the nineteenth century. In 1809, its regular clergy became extinct and the monastery entered a period of decadence, until it was finally abandoned in 1835. In 1850, the building began to be used as a glass factory, which introduced changes in the architectural configuration of the church and the tower. The church was used to house the main oven and the inner floors of the tower were demolished in order to provide space for the drying of glassware. Over the course of the second half of the nineteenth century and the first half of the twentieth century, large areas of the building were demolished. This was probably due to the owners' need for income, which they obtained by selling materials such as marble or stone ashlars. Thus, the eastern cloister, perimetral areas of the main cloister, as well as the sacristy, the apse and the central and the Gospel naves of the church were demolished. The complex reached its peak of decadence when it was used as a pig fattening farm, a situation that lasted well into the twentieth century. In 1964, the building was declared a National Historical and Artistic Monument. This led to consolidation works in 1966. However, the monastery once again suffered severe damages after the 1969 earthquake, involving the complete destruction of one of the columns of the northern wing of the main cloister [13].

Ever since, the building has undergone constant archeological surveys and maintenance works. During the 1970s, the most important interventions regarding the structure of the cloister were carried out: the column that had collapsed after the earthquake was rebuilt using calcarenite stone and the infill over the upper gallery of the northern wing was replaced by a series of concrete beams with the goal of avoiding the collapse of the vaults beneath it. In the 1980s, more improvements were made, of which the introduction of a concrete slab above the infill of the entire first floor stands out [13].

2.2. *Current architectural configuration*

Presently, the eastern cloister and the printing house no longer exist. As for the church, only two chapels of the Epistle wing, the staircase and the wall attached to the main cloister remain standing. So does the tower, albeit with an internal configuration that differs from the original. After being used as part of the glass factory, its interior was almost completely emptied out. Regarding the main cloister (measuring 34.0 x 33.5 m in plan), its lower level has been completely preserved: a composition of semicircular arches that rest on half columns and coffered sail vaults (Fig. 4). Of the upper level, the only remaining elements are the vertical structures, three-centered arches in this case, and some of the vaults in the northern gallery.

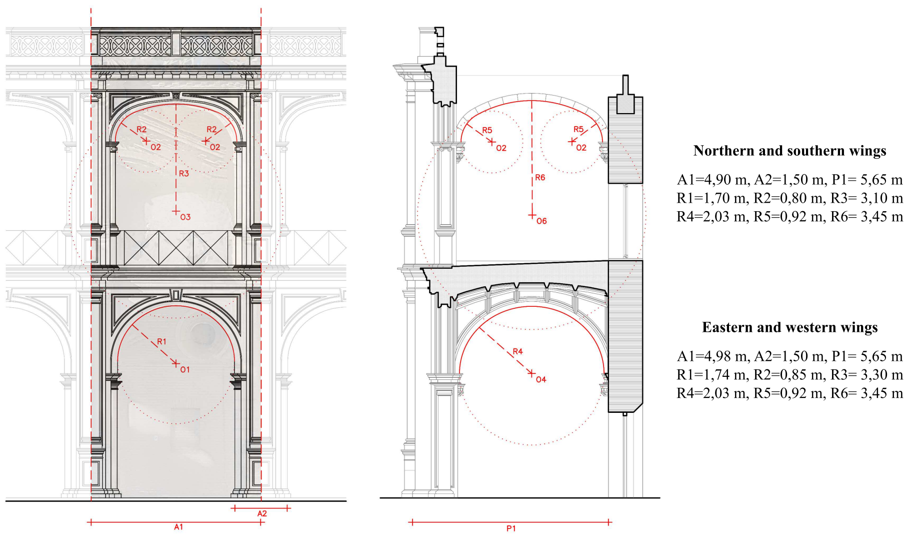

Figure 4: Geometric model of the module type.

Within the base of wings where some of the main spaces of the monastery once stood, along the southern and eastern side of the main cloister, a new building has recently been erected, used as a civic center (Fig. 3.c). In general, this building has a reinforced concrete structure that is not entirely freestanding, since it makes use of the original outer walls of the monastery's galleries as part of its supporting elements (Fig. 5). The result is that, on the one hand, the eastern wing of the new construction is supported by both the existing wall and a line of reinforced concrete columns parallel to it. These columns rest on a linear foundation executed above the remains of the existing foundation. On the other, the southern wing is supported by a load-bearing clay block wall built over the remains of the outer wall of this former wing, and by the existing inner brick wall of the cloister [14].

Figure 5: New building structure: (a) resting on the ancient one; (b) east wing; and (c) south wing.

2.3. Current state of the building

Today, the historical part of the building presents severe damages, which have worsened with the construction of the new building. By comparing the inspections carried out in 2003 [13], that is, before the construction of the new civic centre, with others made since 2013, therefore after the attachment of the new building [15–17], changes in the damage state of the cloister were detected. Thus, por example, current damages such as the longitudinal cracks in the vaults of the north gallery (Fig. 6d), the cracks in the keys of the arches of the ground floor of the east wing (Fig. 6f) or the longitudinal cracks between vaults and eastern wall (Fig. 6e) were not mentioned as detected damages in the 2003 inspection report [13]. The current state shows that the most relevant damage is concentrated along the northern and eastern wings of the cloister. Damages includes cracks and material loss, as illustrated in Figure 6.

Figure 6: Most significant damage: (a) vertical cracks in the north wing columns; (b) section loss in the north wing columns; (c) rebuilt column after the 1969 Portuguese earthquake (Fig. 9 - column 10); (d) longitudinal cracks in the vaults of the ground floor of the north gallery; (e) Longitudinal cracks at the intersection of the vaults with the historic wall of the east wing; and (f) cracks in the keys of the arches of the ground floor of the east wing.

3. Structural inspection of the monastery

A series of techniques were applied to the building with the aim of inspecting the state of its structure, both at a global and at a local level. In this way, a set of mostly non-destructive tests were carried out in order to obtain information regarding the behavior of the structure and the condition of some of its elements.

3.1. Inspection of the structure at a global level

3.1.1. Ambient vibration tests (AVTs) and Operational Modal Analysis (OMA)

With the aim of carrying out a dynamic identification test that could provide information regarding the global behavior of the structure, seven experimental ambient vibration campaigns were carried out on the object of study: four in the cloister of the monastery, one per each of its four wings, two on the wings of the new buildings and, lastly, a general one in order to compare and validate the results of the partial campaigns. Before these campaigns, a study was carried out based on a simplified preliminary model in order to be able to define the relevant measuring points. Figure 7 shows a diagram of the measuring points considered on a generic wing, a diagram that repeats itself on each of the studied wings, resulting in a total of 32 points per campaign. Four accelerometers were used as reference, and another four were placed on each column and walls, taking measurements at two heights: 6.80 m and 12.20 m, coinciding with the first floor level and at the springer line of the upper arches. Accelerations along the two orthogonal directions in plan were recorded with the objective of identifying the vibration modes that could develop longitudinally and transversally on each wing. In this way, a total of 16 measurements were taken in each experimental campaign.

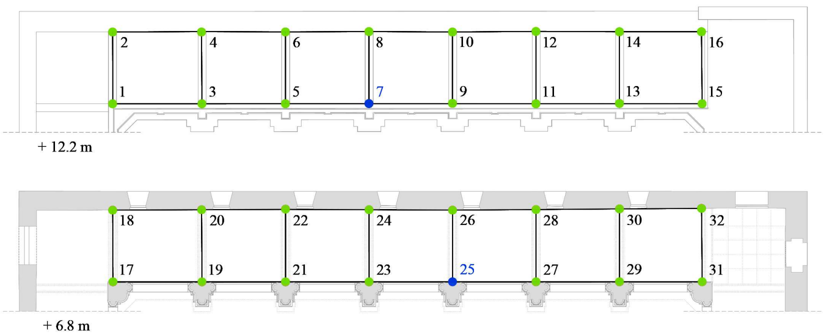

Figure 7: Plan showing the location of the accelerometers (reference accelerometers in blue).

The measuring equipment used to carry out the different ambient vibration tests comprised force balance accelerometers with a bandwidth between 0.01 and 200 Hz, a dynamic range of 140 dB, a sensitivity of 10 V/g and a mass of 0,35 kg (model ES-U2). These accelerometers were connected to a data gathering system with an ADC of 24 bits equipped with anti-alias filters (model GRANITE, by KINEMETRICS). The parameters established for the dynamic tests were a sampling frequency of 100Hz and a duration of 15 minutes per test. Similar temperature and humidity conditions were found during the tests.

The data obtained was processed using the modal identification method known as Enhanced Frequency Domain Decomposition, a method in the frequency domain that is implemented in the ARTeMIS Modal software [18]. Table 1 summarizes the obteined results, including the frequencies associated with each vibration mode, the damping ratios and the standard deviations presented by these values, that is, both of the frequencies and of the damping ratios.

Mode Nº	**Wing**	**EFDD**			
		f (Hz)	**std**(f)	ξ (%)	**std**(ξ)
1	N	2.01	0.02	1.00	0.27
2	W	2.33	0.02	0.86	0.12
3	N, E, S	3.09	0.04	2.17	0.24
4	N, E, S, W	3.35	0.03	0.62	0.31
5	W	3.89	0.04	0.67	0.26
6	N, E, S, W	4.31	0.05	1.56	0.80

Table 1: Modal parameters: natural frequencies (f), damping ratios (ξ) and standard deviation (std).

Likewise, Figure 8 shows the first six vibration modes that were identified, which fall within a frequency range of 0 to 5 Hz. The identified modes correspond for the most part with the bending modes of the different wings of the cloister. The first, second and fifth are local modes, in which only one of the wings undergoes excitation, while the rest of the modes are global modes, in which at least two of the wings undergo excitation under the same frequency value.

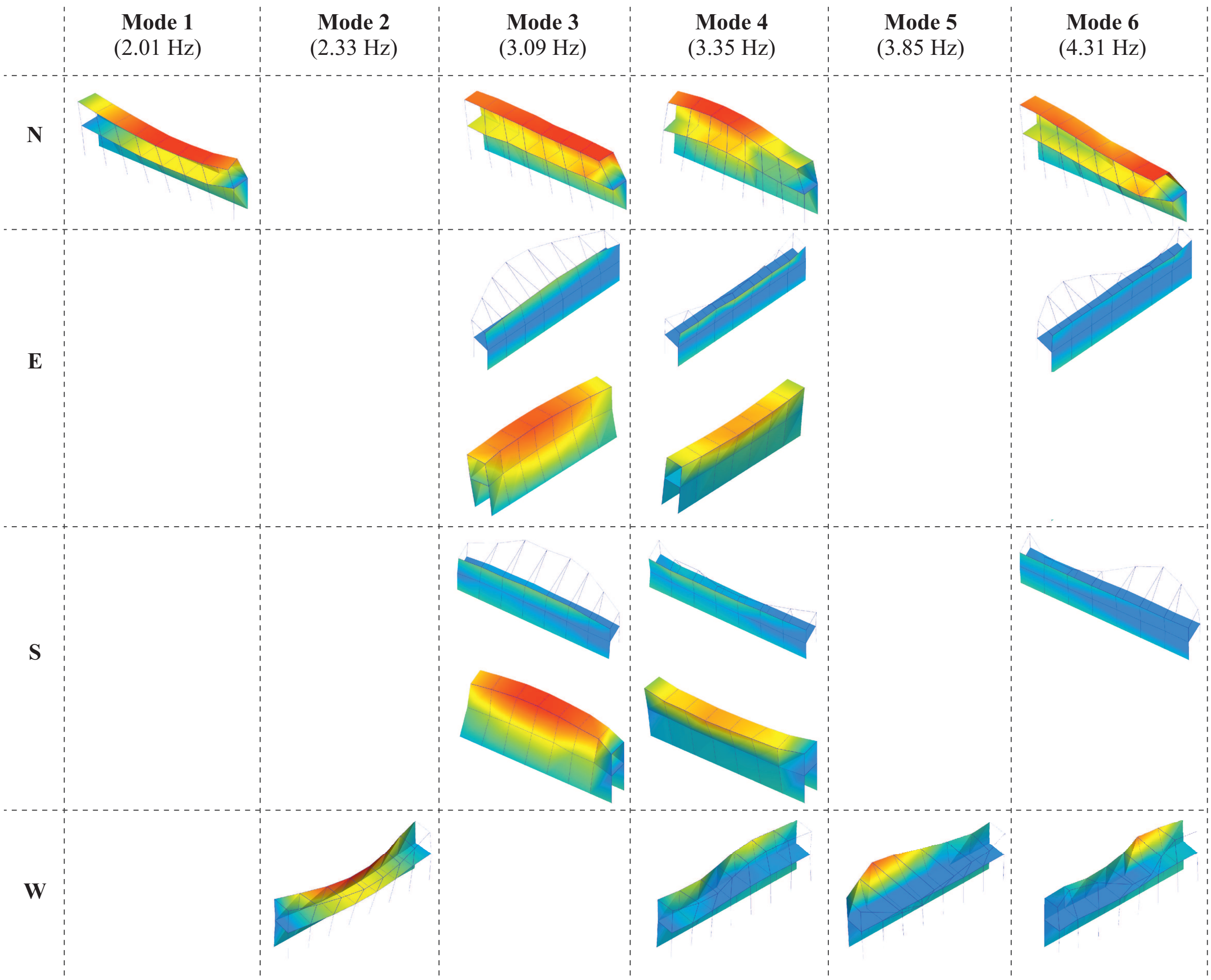

Figure 8: First six experimental vibration modes of the experimental model.

3.1.2. Inspection of damage evolution

Two inspection techniques were carried out in order to establish whether the damages were still active or if the building was mostly stable [19]. On one hand, changes after one year in the position of selected control points were topographically measured (from July 2015 until July 2016) . For this, 87 reflective targets were used. Most of them were placed along the eastern wing, on columns, arches and vaults keystones and the masonry wall. Likewise, other six targets were distributed among columns of the northern, western and southern wings. On the other hand, 11 crack openings were monitored for 15 months (from July 2014 to October 2015). These cracks were located along the eastern wing, at keystones of tranverse arches and on the masonry wall. During 15 months, crack openings were measured on nine different dates. Results of both topographic control of targets and the measurement of crack openings did not reveal an evolution of the deformation state or the damage state of the building.

3.2. Inspection/analysis of the structure at a local level

Given the fact that the areas and elements of the historic building that present the most damage can be detected visually, as commented in section 2.3, these elements were inspected in order to obtain information regarding their state. Next, the most relevant results of this inspection process are described, namely with respect to the columns and foundations of the building (Fig. 9).

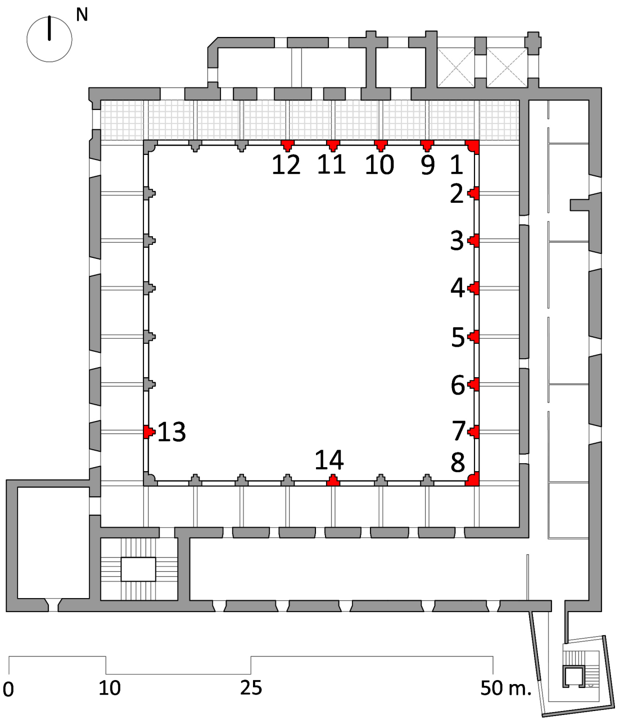

Figure 9: Location of inspected columns.

3.2.1. Inspection of sections

With the aim of determining the internal composition of the sections of the columns of the main cloister and to assess their state, a series of wave propagation tests were carried out. On the one hand, 12 columns on both stories were inspected with the use of a single-frequency 2D georadar (Fig. 9; columns 1-10 and 13-14). In this case, a 2.3 GHz nominal frequency antenna was used with an effective penetration of up to 0.80 m. The radargrams obtained showed that these were solid columns made of a single material. However, inner gaps were detected, but these were only a few centimeters wide and therefore irrelevant, located generally between each block of stone [15] (Fig. 10).

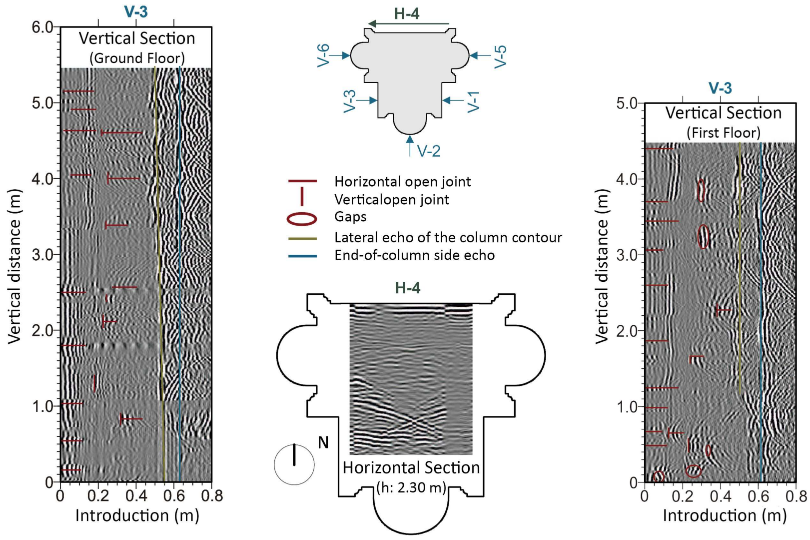

Figure 10: GPR images of column 9 [15].

On the other hand, 10 columns (1-4 and 9-14) were inspected by means of high-resolution seismic tomography with the aim of detecting excessive material degradation. Two horizontal planes of each of these columns were studied, at heights +0.70m and +2.00m. The velocity models obtained present values typical of the calcarenite stone that they are made of, that is, between 1000 and 2000m/s [15]. However, the tomograms show velocities that are generally lower at inferior levels (Fig. 11). Likewise, at the same heights, velocities that are considerably lower (in the order of 30%) in the columns of the northern wing in comparison with the values recorded for those on the southern wing [15]. These results show that there is more material degradation and, therefore, a reduction of capabilities in the areas with a lower associated propagation velocity. There is one exception: the column on the northern wing that was rebuilt. This column presents higher velocity values, reaching up to 1995 m/s at its core.

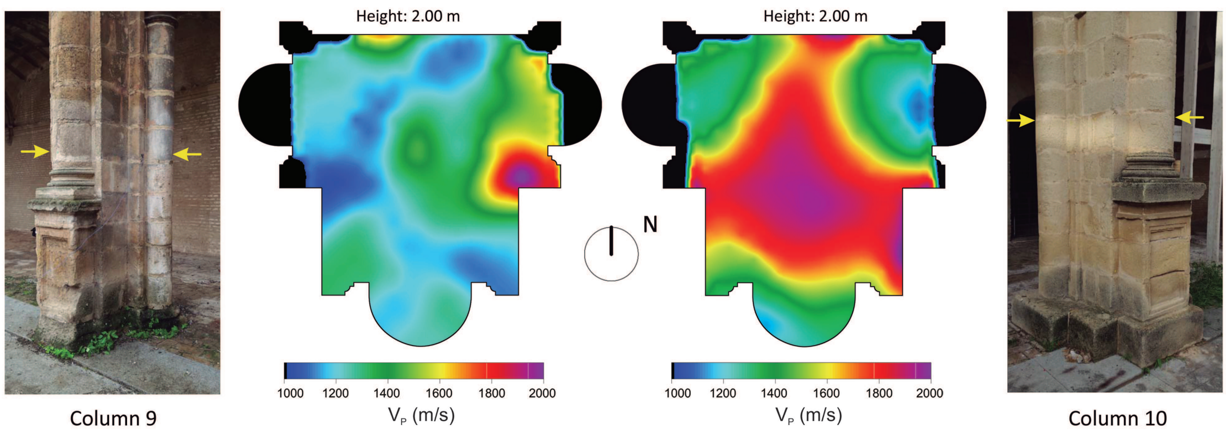

Figure 11: Tomography of columns 9 and 10 [15].

3.2.2. Inspection of the mechanical properties of the materials

In order to assess the available information about the resistant capability of the columns, this study considered a set of uniaxial compressive tests on samples extracted from the original structure. Given the protected nature of the building and the MDT character of the test, very few samples were extracted. In 2003, five samples were tested in accordance to the regulations of UNE 67026/84. Three of them were extrated from columns of the eastern, southern and western wings. On the other hand, two brick masonry samples from the walls of the eastern and southern wings, that is, the walls of the wings that the new civic center is attached to, were also extrated to be tested in the lab [20]. Later, in 2015, two samples were taken from columns 1 and 11 and tested in accordance to UNE-22.950-3 [19].

Regarding the results obtained from samples taken from columns, a compressive strength of around 2.5 MPa was obtained for three of the samples in dry conditions, while the values obtained for the other two were outliers (5.4 Mpa, for column 1, in 2015; and 1.5 Mpa, for the one of the western wing, in 2003). In 2003, samples from columns were tested to also stablish compressive strength in saturated conditions. Values of 1.8 MPa and lower were obtained. Lastly, the Poisson coefficient obtained from tests in 2015 was 0.23 [19].

The number of tests that was performed is reduced to directly use values obtained in the numerical model. However, they provide an initial order of magnitude. Regarding stone masonry structures and despite the dispersion of some results, the most representative ones match those that literature establishes specifically for compressive stresses in this kind of stone, that is, around 2.2 Mpa [19, 21].

The calcarenite stone used for the columns of the cloister was extracted from a nearby quarry (the quarry of San Cristóbal, in El Puerto de Santa María, Cádiz). This type of stone has a very high porosity, typically about 32-39% [22, 23]. Likewise, this stone is characterized by a significant degradation of mechanical properties under increasing water content [16]. This is why the moisture content of the cores of a total of 8 columns at two different heights was obtained: +0.70/0.90 m and +2.00 m. By analyzing the results obtained from these in situ tests , it is possible to state that the moisture content at the lower part of the columns is higher in every case, with an average value of 30%, reaching up to 70% in columns 1 (northern wing) and column 14 (southern wing).

Lastly, *in situ* sonic tests were carried out on the walls and columns with the aim of obtaining the dynamic elastic modulus. On columns, P-waves and S-waves were measured following two horizontal and orthogonal transits at two different heights, +0.70 m and +2.00 m. This is analogously applied on the cross section of walls. At present, the relationship between the dynamic modules and the static modules has yet to be defined for many structural materials, especially those with high porosity, such as the San Cristbal stone [23, 24]. Despite this, the analysis of the results of this non-destructive test can provide information at a qualitative level and enable the detection of alterations. Sonic tests were carried out on a total of 10 columns (1-4 and 9-14) and 8 walls. The results obtained are within the typical range of the materials analyzed, between 2.3 and 5.2 Gpa [25]. However, it is important to highlight the fact that the columns of the northern wing present low elastic modulus values, showing that this is the area in which the material is most altered. The exception is the column of the northern wing that was reconstructed, the elastic modulus values of which was tripled those obtained in the most altered areas. Therefore, based on the tomography and sonic tests, the higher level of degradation of the columns of the northern wing is confirmed. Likewise, this degradation is in accordance with the higher humidity levels detected in this same area.

3.2.3. Inspection of the foundations of the northern wing

Due to the extent and type of damages seen in the supporting elements of the northern wing of the cloister, alterations or deficiencies in their foundations are likely. To study these, Ground Penetrating Radar (GPR) was used as a non-destructive inspection technique. A 29-channel, 3D Multifrequency GeoRadar was used. The pulses were emitted within a frequency range of 100-2500MHz, at intervals of 2.5MHz, measuring depths of up to three meters. In areas in which accessibility with this instrument was not possible, a 2D single-frequency GeoRadar with a 250MHz antenna was used [15].

As a result, the test showed the existence of a series of structures and anomalies. On the one hand, a set of channels was located at a depth of 0.10 m, along with others at a depth ranging between 0.30 and 0.45 m. On the other hand, a possible angled gallery was identified, its layout connecting the courtyard with the entrance into the tower. The gallery appears to be approximately 1 m wide, and located at a depth of 0.30-0.40 m (Fig. 12). Finally, the results indicate the possible existence of tie beams between the foundation elements, albeit in what seems like discontinuous form. Likewise, the reflections indicate that humidity levels are higher in the area around the mentioned tie beams [15].

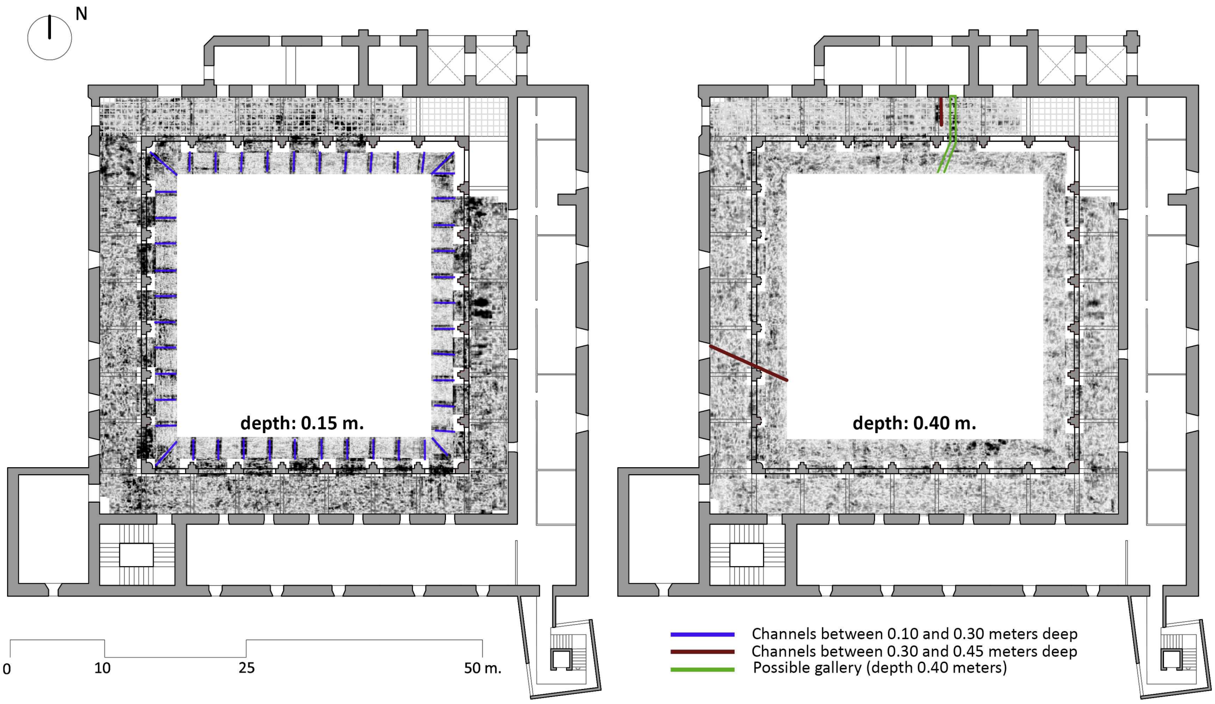

Figure 12: GPR images of foundations (depth: 0.15 and 0.40 m) [15].

Based on the alterations detected with the GPR, a series of moderately destructive tests (MDT) were carried out under the supervision of archaeologists. In this way, on the one hand, 6 inspection pits were dug to examine the foundations, 4 under the columns of the northern wing (1, 9, 10 and 11), and 2 under columns 13 and 14 (of the western and southern wing respectively). On the other, 8 small inspections openings were carried out in the masonry (30x30 cm and 30x90c m) in order to examine the vaults [17]. Of the obtained results, the following stand out:

- In general, each of the columns of the northern wing has its own independent foundation, at a shallow depth. Only part of the bases of the columns, the northern halves, is set upon a strip foundation consisting of the remains of a fifteenth-century brick wall reused for this purpose. This element rests upon a layer of lime mortar. The southern halves of the bases of the columns rest directly on the ground. Only one independent element was constructed, in the form of a shallow foundation, attached to the aforementioned wall and with no tie beams. This element is made of several courses of roughly laid bricks set with low quality mortar (Fig. 13).

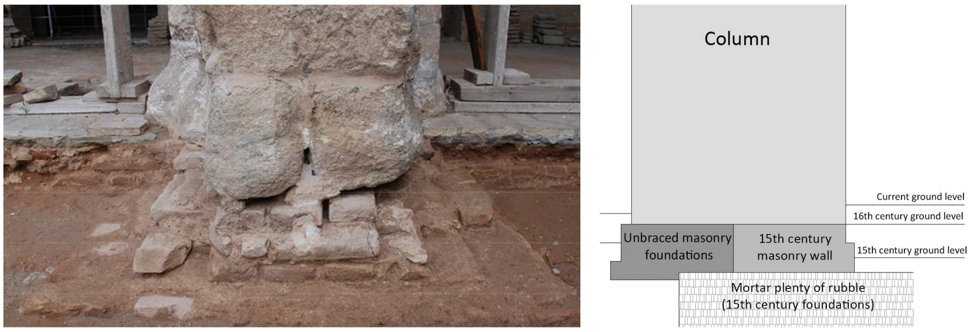

Figure 13: Historical foundations: front view (a) and cross section (b).

- The building system that has been described led to differential settlements between the northern and southern halves of the bases of the columns. According to the archaeologists, this differential settlement reaches up to 2.5 cm (column 11).

- The foundations lack any sort of tying element: (i) the elements under the southern halves of the bases of the columns are not tied to each other and (ii) two elements, introduced most likely in the nineteenth century when the e monastery was used as a glass factory, cut through the main strip foundation: a drain pipe that connects the courtyard with the entrance of the tower (previously detected by the GPR between columns 10 and 11), and an underground vault between columns 1 and 9.

- The system and setting depth of the foundations of the columns on the eastern wing differs from that of the northern wing. The foundation of these columns is deeper and has more consistency. It was built after that of the northern wing and is connected to it at the base of column 1.

3.3. Remarks

Of the different tests performed, the OMA carried out based on the results of the AVTs is the technique capable of providing the most information regarding the global behavior of the structure. The remaining techniques provide information about the state of the elements at a local level, and can be applied extensively when they are non-destructive and do not aggressively affect the heritage asset. However, even though these can be widespread (and costly) campaigns, they do not give information regarding the global behavior of the building. The different inspection campaigns carried out on this building are coherent in their results, broadly coinciding with the deteriorated state and capabilities of the elements of the northern wing. Even though non-destructive tests have unquestionable advantages in the diagnosis of the built heritage condition, they also have their limitations and an adequate diagnosis may require moderate destructive tests . In this case, the detection of differential settlements at the base of the columns of the northern wing due to isolated and deficient foundation elements, along with the existence of a foundation without continuity has been possible thanks to the inspection pits executed with the supervision of archaeologists after the results obtained from the GPR.

4. Structural analysis. Modeling and integration of techniques

Based on the results of the different tests carried out, along with the knowledge acquired regarding the historical evolution and milestones of the monastery, a mathematical model can be developed. This is a finite element model that integrates information gathered experimentally. Even though the main damages on the building, such as the collapse of column 10, were due to seismic forces, the increase in some of these damages and the appearance of others over the course of the last few years took place after the construction of the new civic center and the use of the ancient galleries as circulation areas. It is a cause-effect relationship as no seismic action has been registrated during the period of the construction of the new building, the putting into service of the whole and the increase of damage state [26]. The new configuration of the building implies an increase of vertical loads, both dead and live loads. Thus, to reach the goal (i), that is, to assess the improvement of the numerical model by integrating information obtained experimentally from different disciplines, an analysis under gravitational loads is carried out in such a way that the validation of the model can be done by considering the existing damage.

In order to develop the model, a modal analysis had to be carried out, along with different previous analyses that assumed an elastic and linear behavior of the materials, as explained next. Once defined, the resulting model was subjected to a non-linear analysis, based on which the validity of the model itself was ensured and the structural capacity of the building to gravitational loads was assessed. This analysis was carried out using the Abaqus/CAE software [27].

4.1. Description of the model

The model was constructed using topographical techniques. Likewise, a photogrammetric survey was realized. The latter showed deformations in the arches of the main cloister that have not been considered initially in the numerical model. The aim is to use this information to validate the results of the mathematical model.

Elements and boundary conditions. Concerning the elements taken into account, two different sets are considered. On one hand, those that are part of the structural system of the new civic centre. This is a new system and it is well documented, so the uncertainty about the properties of its elements is lower. Likewise, this system shows no damage and therefore it is not necessary to extract detailed information from it to reach the goals of this study. This allows to use simpler elements and thus to reduce the computational time that is needed to perform the subsequent analysis. In this way, the columns of this system have been modeled using beam elements (type Beam B31- line- 2 node). Likewise, floors, slabs, concrete beams, and the clay block wall have all been modeled using shell elements (type Shell S3R- triangular- 3-node). On the other hand, the elements corresponding to the historical construction were modeled using volumetric finite elements, mainly due to the need to extract from the analysis more detailed results to achieve the proposed objetives. Therefore, and to allow an adequate adjustement to the geometry of the ancient cloister, Solid C3D4 elements were applied (first order reduced integration tetrahedral 4-node elements). The model has a total of 15.9M elements, 3.0M nodes and 9.6M degrees of freedom (Fig. 14).

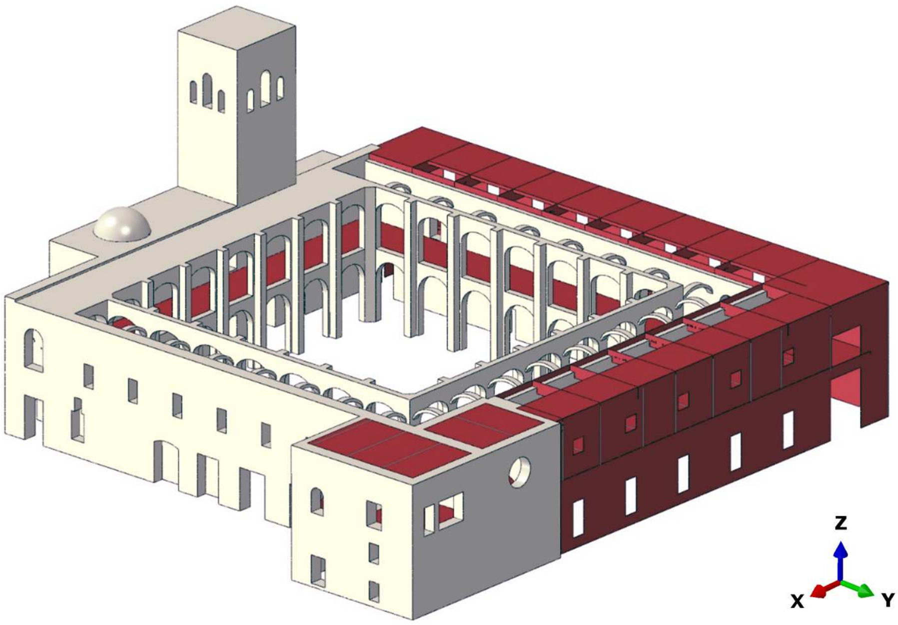

Figure 14: Three-dimensional FE model of the monastery (mesh with 15.M elements not shown).

With respect to the boundary conditions, initially the movement of the nodes situated at the base of the supports was considered fixed. However, given the differential settlements detected during the surveys (section 3.2.3 and Fig. 13), a preliminary linear analysis of the model was carried out in order to assess the influence that considering these settlements would have on the results. This study revealed that taking into consideration these settlements in part of the supporting surface area of the columns was relevant to the analysis, since it entailed significant changes in their structural behavior. Figure 15 shows the results from this preliminary study from a qualitative point of view. In this study, only columns 1,9 and 11 were subjected to the mentioned settlement by an imposed downward displacement of 2cm, while the base of column 10 was completely fixed. As it can be observed, the consideration of the settlement along half the base of the column implies changes in the position of the more compressed areas on the column. Thus, in column 10, the highest compressive stresses are found in the lower areas of the outer face and in the upper areas of the inner face, while the highest compressive stresses of the rest of the columns are located along the inner face. In correspondence with results from archaeological inspections (section 3.2.3) and taking into consideration the results from the preliminary linear analysis mentioned above, differential settlements as those described were considered in the model at the base of columns of the northern wing. Thus, nodes at the half-base of each column that were next to the gallery were considered fixed, while those of the other half counted on imposed downward displacements. The boundary conditions of each column in the northern wing have been modeled as described with the exception of column 10 (rebuilt).

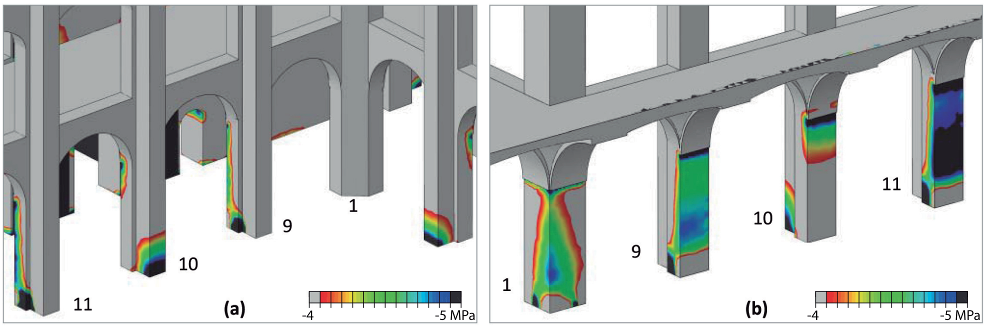

Figure 15: Exterior (a) and interior (b) views from preliminary model with differential settlements only on columns bases 1, 9 and 11. A different structural behaviour of column 10 (without settlement) with respect to the other columns can be observed regarding compressive stresses.

Materials and mechanical properties. In the part of the model that corresponds with the historical building, the different materials have been modeled in accordance to both the inspections carried out (Section 3.2) and the information extracted from previous visual inspections and archaelogical studies [13, 16, 17]. In this way, different layers have been adopted for the floor system and for the load bearing walls, with the exception of a rammed earth wall in the eastern wing, which has been considered as a single material. The main goal of this study refers to the improvement of the model results at a local level, so a more detailed model was developed in order to obtain more detailed results. The use of volumetric finite elements for multi-layer systems allowed both a better adjustement to the actual geometry of the structure and a higher degree of fidelity regarding the way load bearing works between structural elements. Thus, the floor system has been modeled with a curved lower layer of stone masonry (vaults), an upper horizontal slab and an infill which is set between them. On the other hand, bearing walls has been modeled with three layers, the outer ones as brick masonry and the inner one as an infill. The columns have been considered as solid stone masonry elements (Fig. 16).

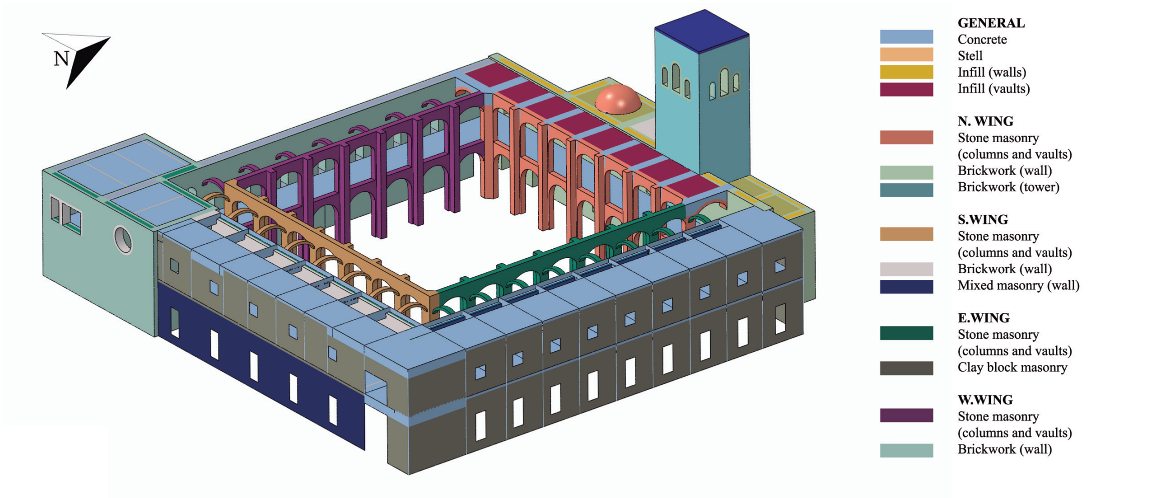

Figure 16: Materials used in the updated FE model.

On the one hand, density, Poisson's ratio and compressive strength are obtained from bibliographical data [15, 20, 21, 28] and according to results from compressive tests assessed in section 3.2.2., as shown in Table 2. The estimation of low compressive strength values of the stone masonry stand out, at 2.0 MPa. This value is coherent both with the most representative ones obtained from the compressive tests carried out, and with the reduction of the capabilities that this type of stone suffers with high humidity indexes, like those that have been detected (section 3.2.2.). On the other hand, the elastic modulus of the constituting materials is obtained by means of a process by which the model is calibrated. In this process, the aim is to reach the dynamic response of the model, obtained through a modal analysis, to adjust to the dynamic response of the real structure, which has been obtained experimentally with AVTs and OMA (section 3.1.1). In this way, the elastic modules are obtained from their consideration as updating parameters in this calibration process. The aim is to have a calibration regarding two criteria: the modal shapes and the associated frequencies.

	Material	**Density** (kg/m^3)	**Young's modulus** (MPa)	**Poisson's ratio**	**Compressive strength** (MPa)
General	Concrete	2500	23000	0.23	25.0
	Steel	7850	210000	0.23	223.0
	Infill (walls)	1500	500	0.23	0.9
	Infill (vaults)	900	35	0.23	0.8
N. wing	Stone masonry (columns and vaults)	1800	1200	0.23	2.0
	Brickwork (wall)	1800	1000	0.23	1.8
	Brickwork (tower)	1800	2200	0.23	2.4
S. wing	Stone masonry (columns and vaults)	1800	1500	0.23	2.0
	Brickwork (wall)	1800	1200	0.23	0.9
	Mixed masonry (wall)	2200	4000	0.23	1.4
E. wing	Stone masonry (columns and vaults)	1800	1000	0.23	1.8
	Clay block masonry	2000	4000	0.23	3.2
	Rammed earth	1400	700	0.20	0.9
W. wing	Stone masonry (columns and vaults)	1800	1500	0.23	2.0
	Brickwork (wall)	1800	1000	0.23	1.8

Table 2: Material properties used in the updated FE model.

Model calibration process. The initial idea was to calibrate the model using just one value of the elastic modulus per material, regardless of the wing of the building it was in. However, the adjustment of the model was unsatisfactory according to the two calibration criteria that had been defined. To achieve an adequate calibration, different elastic modules had to be taken into consideration for the same material depending on the wing it was located in. This consideration was backed by supplementary data from two different sources. The first is the archaeological study of Monastery, which estimates that the construction of the different wings of the cloister took place in different periods up to 150 years apart [13]. The second are the experimental campaigns that were carried out: (i) the results provided by the high-resolution seismic tomography show different levels of deterioration depending on the wing; (ii) the sonic tests likewise show different values for the dynamic elastic modulus for the different wings. Table 3 relates the experimental and numerical values of the frequencies corresponding with the vibration modes identified. It confirms the high level of adjustment that occurs, with MAC values between 0.88 and 0.99, for all of the vibration modes. Here, f_{EFDD} are the frequencies obtained from AVT, $f_{NUM.MODEL}$ are the frequencies from the numerical model, the difference is measured with respect to the experimental frequency and MAC is the Modal Assurance Criterion, a statistical indicator that measures the difference between eigen-modes (usually accepted as coherent if it is higher than 0.70) [6].

	Experimental model vs. Numerical model					
	Mode 1	**Mode 2**	**Mode 3**	**Mode 4**	**Mode 5**	**Mode 6**
f_{EFDD} (Hz)	2.01	2.33	3.09	3.35	3.86	4.31
$f_{NUM.MODEL}$ (Hz)	2.01	2.33	2.97	3.37	3.73	4.15
% Dif.	0.00	0.00	3.88	0.54	3.32	3.73
MAC	0.99	0.99	0.95	0.95	0.98	0.88

Table 3: Comparison between experimental and numerical eigen-frequencies.

In addition to the model calibration based on eigen-frequencies, the adjustment of modal shapes was also achieved for the six first modes. As an example, Figure 17 relates the modal shape obtained numerically and experimentally for the fourth vibration mode. This figure shows bending modes along the four wings. The correlation between both numerical and experimental results can be observed even for inflexion points.

On the other hand, and in addition to the adequate adjustment obtained, the values of the elastic modules acquired (Table 2) have been validated based on: (i) the range of the values of the material itself [28]; (ii) the dynamic elastic modules from the sonic testing, with the northern wing showing the lowest elastic modules, the southern wing the highest and the eastern and western wings intermediate and matching levels; (iii) the results of the high-resolution seismic tomography, which indicate a higher degree of deterioration in the columns of the norhern wing.

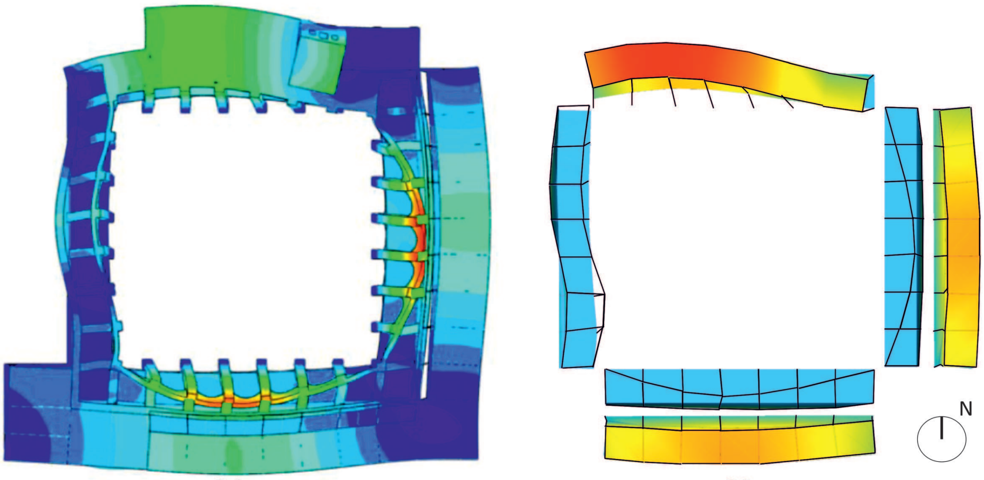

(a) (b)

Figure 17: Modal shape, fourth vibration mode. Numerical model (a) vs Experimental model (b).

Constitutive model. Given the cracked state of the structure, and that one of the goals is to globally analyze the structural capacity of the building, a constitutive model available in ABAQUS software and known as Concrete Damage Plasticity (CDP) material model was adopted [27, 29]. Despite being a model conceived to model fragile isotropic materials such as concrete [29], its use has been extended to the modeling of masonry based on the consideration of an isotropic macro-model and since it allows the definition of materials with different compressive and tensile strengths as well as different failure mechanisms, that is, tensile cracking and compressive crushing. Some recent applications of this constitutive model to the structural analysis of historical masonry constructions can be found in [3, 30–34].

In these kinds of models, beside the aforementioned defined values, those that correspond to the fracture energy and tensile strength must also be included. The values corresponding to both parameters have been taken from bibliographical references. Therefore, as fracture energy values we have used 0.02 KPa/m for the stone masonry and for the brickwork [35, 36]. As for tensile strength, the use of low values must be pointed out in order to generate a model that is weak to tensile forces. In general, 50 KPa has been considered, with values that are lower for the in-fill materials of walls and vaults, as well as for the rammed earth walls, in this case 40 KPa [37–39].

Consideration of the construction phases in the analysis. In order to assess the need to consider the different construction phases of the building, a preliminary structural analysis was carried out that assumed an elastic and linear behavior of materials and which took into consideration the stiffness of the building as a whole, including the new civic center.

The results showed concentrations of stresses and strains that did not correspond with reality. The main reason for this is that the low values identified for the elastic modulus cause great shortenings of the elements due to axial stresses [40]. These shortenings alter the stress and strain state of the areas closer to them. The elements that suffer this the most are those located between the tower and the northern gallery, as well as those between the cloister and the new civic center. Thus, for example, this previous model showed a very high level for tensile stresses at the base of the arches that belong to the cloister's lower level and that are closer to the tower. The mentioned shortenings are different for the tower wall and for the columns, so it implies different displacements at the bases of the arches between them. This leads to aditional tensile stresses at the mentioned areas that do not correspond with reality.

In addition, as mentioned, the monastery was built over the course of a drawn-out period and has been subjected, throughout its history, to unique milestones, such as the loss and reconstruction of one of its columns. Therefore, the results extracted from a model defined by construction phases with staggered increases of stiffness are of greater value. These phases have been defined according to the information provided by the archaeological studies of the monastery [28]. Figure 18 defines the 6 steps that have been taken into consideration as phased analysis.

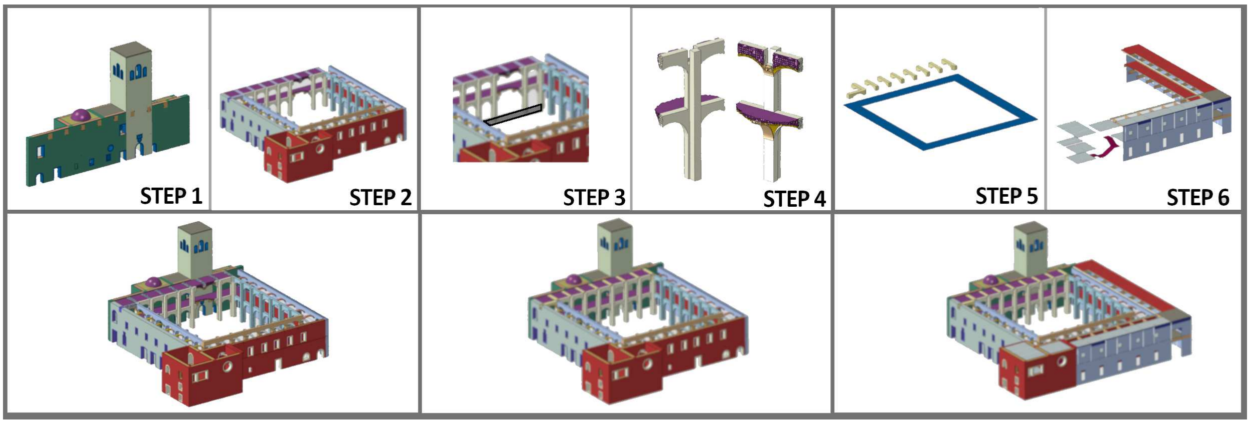

Figure 18: Construction phases taken into consideration in the analysis: STEP1, tower, staircase and chapels; STEP2, preserved elements of the cloister without the column lost during the earthquake; STEP3, differential settlements in the columns of the northern wing; STEP4, inclusion of the reconstructed column; STEP5, concrete beams and slabs introduced in consolidation works; STEP6, inclusion of the new building.

Consideration of loads. As pointed out, the behavior of the building subjected to gravitational loads has been analyzed. In this model, the self-weight of the structure has been considered, which has been introduced in each of the numerical phases defined, gradually and in different steps, in such a way that the weight is fully introduced in one step of the analysis before proceeding onto the next step. Once the total load is introduced in the last step of the analysis, said load is increased until the system collapses, with the aim of analyzing its capabilities.

4.2. Remarks

The model created integrates specific data extracted from the results of the inspection campaigns that have been carried out. Based on previous structural analyses mentioned in section 4.1, those that assumed an elastic and linear behavior of materials, the influence that the incorporation of this information has on the results of the analysis at a local level has been demonstrated. In the case of the differential settlements, their consideration or not in the model involves an important variation in the results. The calibration of the model based on AVTs and OMA ensures that it maintains a global behavior in accordance with the actual structure despite the introduction of the aforementioned local singularities. Part of the data obtained from the inspection techniques has been incorporated directly into the model. Another set of data, however, is used as complementary information in the definition and/or validation of the intervening parameters.

5. Results

In a first step, the analysis of the results obtained for the historic building as a whole, before including the civic center, allows to verify that the model already shows that the northern wing presents a level of damage above that of the rest of the complex. Damage is located mainly on the keystones of the arches and the vaults, as well as at the base of the columns. The results provided by the model strengthen the hypothesis that the reason behind the collapse of column 10 during the 1969 earthquake was mainly due to the vibrations of the tower. This is so because the results show a tendency of the tower to bend towards the interior of the cloister and a higher level of damage on its northern facade in the vicinity of the existing large niche.

Regarding the eastern and western wings, the model shows that they behave differently in spite of having the same geometric layout. The fact that the wall of the eastern wing is made out of rammed earth, in contrast with the corresponding wall on the western wing, which is brickwork, explains why the former is more affected, even before incorporating the civic center into the model. The model shows that the wall of the eastern wing tends to move towards the east, opening up the structure that supports the gallery. This is in line with the most pronounced damages presented by the arches of the upper floor of this wing. Likewise, and still within this tendency to open up, in this state, the structural model manages to identify damages compatible with the separation crack that exists in the eastern wing between the vaults of the first floor and the wall (Fig. 19). The southern wing, on its part, presents a continuity of material throughout its wall, along with less openings. The model shows that, in general, it holds up better, even though it also detects that the supporting structure of the gallery tends to open up, that is, a displacement of the aforementioned wall towards the south and of the columns towards the north.

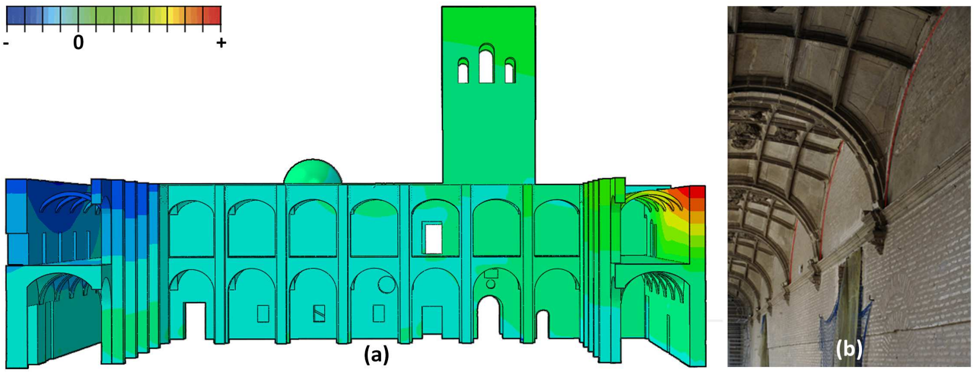

Figure 19: Section though West and East wings (a); Displacements along the X axis (b) and cracks between vaults and wall in the East wing.

In order to obtain these results, specific for each wing and in line with the main damages present in the building, it has been important to identify the properties of the constituting materials for each of the wings. Therefore, for example, the consideration of the rammed earth in the eastern wall has been crucial in order for the model to show its distinct behavior with respect to the western wing, as mentioned. Likewise, in order to obtain the results for the northern wing, it has been equally important to include a building phase in which the column that collapsed was not present and to take into consideration the differential settlements at the base of the columns of this wing. The introduction of these settlements makes the model show incipient hinging of the arches of the northern wing, which becomes greater in the arches adjacent to the missing column. In addition, the introduction of the differential settlements at the base of the columns is the key for the model to show the damage that runs longitudinally along the vaults of the first floor (Fig. 20).

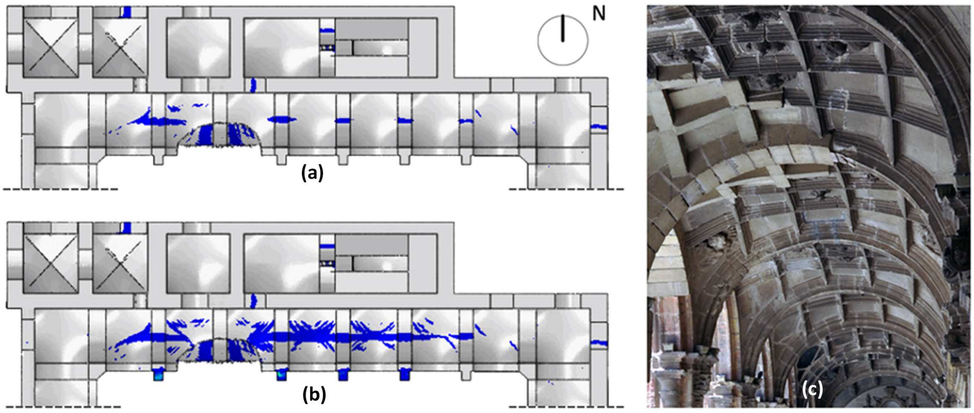

Figure 20: North wing: Damage areas before (a) and after (b) considering differential settlements; (c) Cracks along vaults.

Moreover, the results indicate that the construction of the civic center accentuates aspects of the structural behavior of the cloister that were already incipient before the construction of the new building. The most relevant are: (i) the development of hinges in the keystones of the arches of the first floor, and not only those of the northern wing (Fig. 21); (ii) the displacement towards the east both of the eastern wing wall and of the eastern side of the northern gallery; (iii) the opening up of the supporting structure of the southern wing, that is, the movement of the wall towards the south and of the columns towards the north.

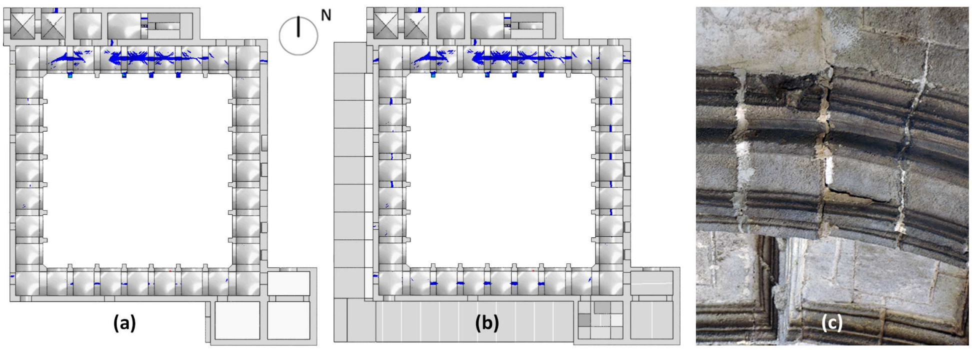

Figure 21: Increase of damage in the keystones of arches after introducing the new civic center: Views from below the historical construction, with past (a) and current architectural configuration (b), and example of cracks in an arch keystone (c).

An analysis of the correspondence between the results obtained numerically and the damage that the actual structure presents demonstrates, on the one hand, that the model is capable of showing the most relevant damage once the step in which the civic center has been concluded (i.e. once the complex is fully introduced into the model with its corresponding self-weight). On the other hand, by increasing the load to determine the collapse, the model shows damage areas that coincide not only with those where the building presents cracks of importance, but even areas were minor cracks exist (Fig. 22). This occurs when a load that is 1.5 to 2.0 times that of the self-weight of the structure is introduced. Finally, if a load of 2.15 times the self-weight of the structure is applied, the same reaches a state of collapse due to the failure of the tower.

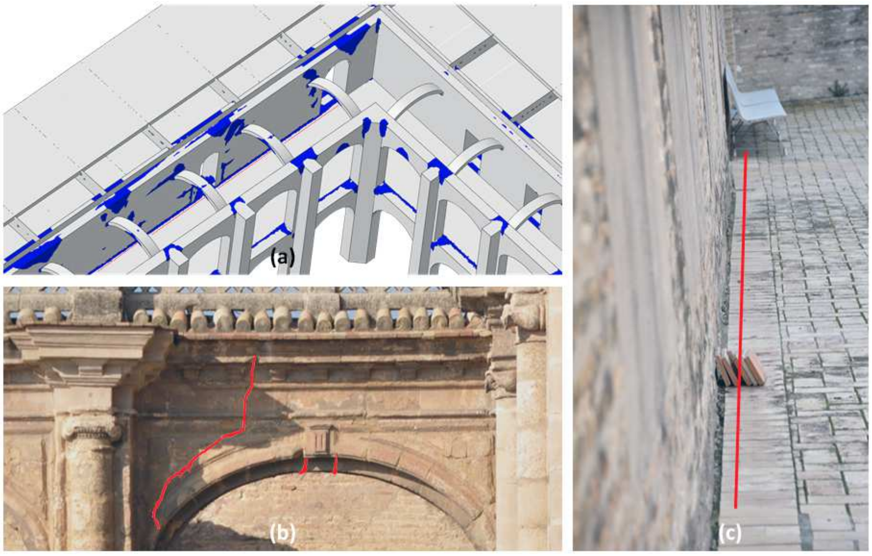

Figure 22: Additional damages on the West wing: model results and current state of the building.

6. Conclusions

This study carried out on the Monastery of San Jernimo in Seville has demonstrated that the incorporation of information from other disciplines other than architecture and structural engineering in numerical structural models helps to improve the results obtained from them. This improvement is based on the generation of a model that is truer to the reality of the building both at a global and at a local level.Therefore, disciplines such as geophysics, archaeology and topography have been crucial in the execution of the advanced structural analysis model.

To achieve a high level of correspondence between the model and reality , the results of some of the experimental tests that were carried out have been incorporated directly into the model. These are: the composition of structural elements (from GPR and topography), values of the elastic modulus of materials (calibration of the model based on the results obtained by means of OMA), or construction phases and differential settlements (archaeology). On the other hand, results provided by other tests have been used to validate the model itself. These have been sonic testing, moisture content tests, photogrammetric surveys, archeological data or visual inspection. Destructive tests from a reduced number of samples to determine the resistance of stone masonry and brickwork have provided dispersed data. This led to the estimation of compressive strength values mainly based on bibliographical sources, to which the more representative values obtained by the compression tests carried out were added. Likewise, looking at the dynamic characteristics of the compound, it can be observed that the parameters introduced locally improved the results in the areas affected by them without significantly influencing the global behavior of the structure of the building.

The structural model has been subjected to a non-linear analysis under gravitational loads until reaching the ultimate load of the structure. It is a detailed model that involves a high computational cost, taking, moreover, into account the need to consider the non-linearity of materials. However, the relatively fine detailing of the model was necessary to reach the goals set out in this study, which included the incorporation and comparison of the results with the information extracted from reality, and therefore, not simplified data.

Regarding the structural behavior of the building, the numerical analysis shows damages in the historical building before the incorporation of the civic center, mainly in the arches, vaults and columns of the northern wing, which appears as the most deteriorated area. The results show that, when the new building was raised and the existing structure of the monastery was used to support it, the damages were accentuated in the form of a generalized hinging of the keystone of the arches or the opening of the supporting structures of the eastern and southern galleries of the cloister.

Subjecting the entire complex to a gravitational load of 1.0g, damage areas are recognized in the model that correspond with the areas in which the historical building presents its main pathologies. For values between 1.5 and 2.0g, the model shows damages that are in line with the areas in which the building shows cracks of lesser importance. This indicates a high level of approximation between the results obtained in this calculation phase and the state that the actual structure presents. Finally, by analyzing the results when the ultimate load (2.15g) is reached, as observed, this collapse is caused by that this collapse is caused by the tower, with additional resistance remaining in the volume that constitutes the cloister.

It is worth mentioning that other assessments will be carried out using the obtained numerical model once it has been validated. Thus, it will be important for this building to develope a safety assessment under seismic loading. Likewise, a continuous dynamic monitoring could be carried out. This would make it possible to detect changes in the damage state by taking into consideration changes in dynamic response of the structure. On the other hand, results from this monitoring could be used to validate a simulation of the environmental effects on the numerical model and further assess the importance of considering these environmental parameters in safety assessments of this structure.

ACKNOWLEDGMENTS

Thanks to the Town Planning Department of the Seville City Council and particularly to Architect Fernando Sánchez Navarrete. This work would not have been possible without their support.

BIBLIOGRAPHY

References

[1] A. M. D'Altri, V. Sarhosis, G. Milani, J. Rots, S. Cattari, S. Lagomarsino, E. Sacco, A. Tralli, G. Castellazzi, S. de Miranda, Modeling strategies for the computational analysis of unreinforced masonry structures: Review and classification, Archives of Computational Methods in Engineering (aug 2019). doi:10.1007/s11831-019-09351-x.

[2] S. Atamturktur, J. A. Laman, Finite element model correlation and calibration of historic masonry monuments: Review, The Structural Design of Tall and Special Buildings 21 (2) (2010) 96–113. doi:10.1002/tal.577.

[3] V. Compán, P. Pachón, M. Cámara, P. B. Lourenço, A. Sáez, Structural safety assessment of geometrically complex masonry vaults by non-linear analysis. The Chapel of the Würzburg Residence (Germany), Engineering Structures 140 (2017) 1–13. doi:10.1016/j.engstruct.2017.03.002.

[4] R. Aguilar, R. Marques, K. Sovero, C. Martel, F. Trujillano, R. Boroschek, Investigations on the structural behaviour of archaeological heritage in Peru: From survey to seismic assessment, Engineering Structures 95 (2015) 94–111. doi:10.1016/j.engstruct.2015.03.058.
[5] C. Gentile, A. Saisi, Operational modal testing of historic structures at different levels of excitation, Construction and Building Materials 48 (2013) 1273–1285. doi:10.1016/j.conbuildmat.2013.01.013.
[6] L. F. Ramos, R. Aguilar, P. B. Lourenço, S. Moreira, Dynamic structural health monitoring of Saint Torcato church, Mechanical Systems and Signal Processing 35 (1-2) (2013) 1–15. doi:10.1016/j.ymssp.2012.09.007.
[7] M. Diaferio, D. Foti, V. Sepe, Dynamic identification of the tower of the provincial administration building, bari, italydoi:10.4203/ccp.86.2.
[8] D. Foti, Non-destructive techniques and monitoring for the evolutive damage detection of an ancient masonry structure, Key Engineering Materials 628 (2014) 168–177. doi:10.4028/www.scientific.net/KEM.628.168.
[9] M. Diaferio, D. Foti, F. Potenza, Prediction of the fundamental frequencies and modal shapes of historic masonry towers by empirical equations based on experimental data, Engineering Structures 156 (2018) 433–442. doi:https://doi.org/10.1016/j.engstruct.2017.11.061.
[10] A. Campos-Costa, L. Ramos, P. B. Lourenço, G. D. Roeck, Damage identification in masonry structures with vibration measurements (2008) 311–319doi:10.1201/9781439828229.ch35.
[11] Á. Bautista-Castro, L. J. Sánchez-Aparicio, P. Carrasco-García, L. F. Ramos, D. González-Aguilera, A multidisciplinary approach to calibrating advanced numerical simulations of masonry arch bridges, Mechanical Systems and Signal Processing 129 (2019) 337–365. doi:10.1016/j.ymssp.2019.04.043.
[12] M.-G. Masciotta, J. C. Roque, L. F. Ramos, P. B. Lourenço, A multidisciplinary approach to assess the health state of heritage structures: The case study of the church of monastery of jerónimos in lisbon, Construction and Building Materials 116 (2016) 169–187. doi:doi:10.1016/j.conbuildmat.2016.04.146.
[13] F. Pozo, R. Gil, E. Méndez, Intervención arquitectónica puntual en Monasterio de San Jerónimo de Buenavista (Sevilla), Consejería de Urbanismo. (2003).
[14] J. García-Tapial, . F Sánchez, Proyecto de Rehabilitación del Monasterio de San Jerónimo de Buenavista para su adecuación a Centro Cívico, Servicio de Rehabilitación y Renovación Urbana (2004).
[15] CEMOSA, Estudio Geofísico mediante Geo-radar 3D Multifrecuencia, Geo-radar 2D y Tomografía Ultrasísmica en la solera y en doce de los Pilares del claustro del Monasterio de San Jerónimo (Sevilla), Tech. rep., Geofísica Consultores (2014).
[16] V. Compán, Informe sobre análisis estructural del Monasterio de San Jerónimo de Buenavista (Sevilla), Tech. rep., Gerencia de Urbanismo de Sevilla (2015).
[17] F. Pozo, Memoria Final. Control arqueológico de calicatas de auscultación en cimentaciones y bóvedas del claustro del Monasterio de San Jerónimo de Buenavista (Sevilla)., Tech. rep., Gerencia de Urbanismo de Sevilla (2014).
[18] S. V. Solutions, Artemis modal 5.0. User's Guide (2015).
[19] CEMOSA, Estudio patológico en el claustro del Monasterio de San Jerónimo (Sevilla), Tech. rep., Geofísica Consultores (2015).
[20] VORSEVI, Ingeniería y Control de Calidad, Estudio de reconocimiento de una edificacin. Monasterio de San Jerónimo (Sevilla), Tech. rep., Gerencia de Urbanismo de Sevilla (2003).
[21] A. B. Padura, J. B. Sevilla, J. G. Navarro, Bearing capacity diagnosis of santiago church (jerez de la frontera, spain), Construction and Building Materials 25 (5) (2011) 2519–2527. doi:doi:10.1016/j.conbuildmat.2010.11.090.
[22] M. A. Bello, A. Martín, Microchemical characterization of building stone from Seville Cathedral, Spain, Archaeometry 34 (1) (1992) 21–29. doi:10.1111/j.1475-4754.1992.tb00473.x.
[23] J. Baeza, V. Compán, M. Cámara, P. Pachón, G. Castillo, Identificación de las propiedades mecánicas de la piedra de San Cristobal mediante técnicas no destructivas, in: REHABEND 2018 on Construction Pathology, Rehabilitation Technology and Heritage Management, 2018.
[24] V. Brotons, R. Tomás, S. Ivorra, A. Grediaga, J. Martínez-Martínez, D. Benavente, M. Gómez-Heras, Improved correlation between the static and dynamic elastic modulus of different types of rocks, Materials and Structures 49 (8) (2015) 3021–3037. doi:10.1617/s11527-015-0702-7.
[25] V. Brotons, Propiedades físicas y mecánicas de una calcarenita: La piedra de San Julián, Ph.D. thesis, Universidad de Alicante (2014).
[26] Instituto andaluz de geofisica (Oct. 2020).
URL `https://iagpds.ugr.es/`
[27] S. Dassault Systemes, Abaqus/CAE 6.13 User's Guide (2015).
[28] N. Augenti, F. Parisiand, E. Acconcia, MADA: online experimental database for mechanical modelling of existing

masonry assemblages, in: 15th World Conference on Earthquake Engineering, 2012.
[29] J. Lubliner, J. Oliver, S. Oller, E. Oñate, A plastic-damage model for concrete, International Journal of Solids and Structures 25 (3) (1989) 299–326. doi:10.1016/0020-7683(89)90050-4.
[30] M. Valente, G. Milani, Seismic assessment of historical masonry towers by means of simplified approaches and standard FEM, Construction and Building Materials 108 (2016) 74–104. doi:10.1016/j.conbuildmat.2016.01.025.
[31] G. Castellazzi, A. M. D'Altri, S. de Miranda, F. Ubertini, An innovative numerical modeling strategy for the structural analysis of historical monumental buildings, Engineering Structures 132 (2017) 229–248. doi:10.1016/j.engstruct.2016.11.032.
[32] M. Valente, G. Milani, E. Grande, A. Formisano, Historical masonry building aggregates: advanced numerical insight for an effective seismic assessment on two row housing compounds, Engineering Structures 190 (2019) 360–379. doi:https://doi.org/10.1016/j.engstruct.2019.04.025.
[33] M. Valente, G. Milani, Damage assessment and partial failure mechanisms activation of historical masonry churches under seismic actions: Three case studies in mantua, Engineering Failure Analysis 92 (2018) 495–519. doi:https://doi.org/10.1016/j.engfailanal.2018.06.017.
[34] M. Valente, G. Milani, Advanced numerical insights into failure analysis and strengthening of monumental masonry churches under seismic actions, Engineering Failure Analysis 103 (2019) 410–430. doi:https://doi.org/10.1016/j.engfailanal.2019.05.009.
[35] G. Brandonisio, G. Lucibello, E. Mele, A. D. Luca, Damage and performance evaluation of masonry churches in the 2009 L'Aquila earthquake, Engineering Failure Analysis 34 (2013) 693–714. doi:10.1016/j.engfailanal.2013.01.021.
[36] S. Casolo, G. Milani, G. Uva, C. Alessandri, Comparative seismic vulnerability analysis on ten masonry towers in the coastal Po Valley in Italy, Engineering Structures 49 (2013) 465–490. doi:10.1016/j.engstruct.2012.11.033.
[37] L. Miccoli, D. V. Oliveira, R. A. Silva, U. Mller, L. Schueremans, Static behaviour of rammed earth: experimental testing and finite element modelling, Materials and Structures 48 (10) (2014) 3443–3456. doi:10.1617/s11527-014-0411-7.
[38] K. Krausz, Tragverhalten gemauerter tonnengewlbe mit stichkappen (2002). doi:http://dx.doi.org/10.18419/opus-165.
[39] P. J. B. B. Lourenço, Computational strategies for masonry structures (1997).
[40] D. Villegas, V. Compán, M. Cámara, Análisis estructural de la Torre del Homenaje de la Alhambra de Granada (España), Informes de la Construcción 66 (Extra-1) (2014) m017. doi:10.3989/ic.13.101.